Investigating the Structural and Magnetic Properties of Nickel Oxide Nanoparticles Prepared by Precipitation Method

Karrar H. Musa

Department of Physics, College of Education for Pure Science (Ibn-AL-Haitham),University of Baghdad, Baghdad,Iraq.
karrar.Hadi1204a@ihcoedu.uobaghdad.edu.iq

Tagreed M. Al- Saadi

Department of Physics, College of Education for Pure Science (Ibn-AL-Haitham),University of Baghdad, Baghdad,Iraq.
taghreed.m.m@ihcoedu.uobaghdad.edu.iq

Abstract

This work used the deposition method to synthesize nickel oxide nanoparticles. The materials mainly used in this study were nickel sulfate hexahydrate (as a precursor) and NaOH (as a precipitant). The properties of the nanopowder were characterized by XRD, FE-SEM, EDX, and VSM. The obtained results confirmed the presence of nickel oxide nanoparticles with a face-centered cubic (FCC) structure with a lattice constant (a=4.17834 Å). Scherer and Williamson-Hall equations were used to calculate the crystallite size of about (30.5-35.5) nm. The FE-SEM images showed that the particle shape had a ball-like appearance with a uniform and homogeneous distribution and confirmed that the particles were within the nanoscale. The presence of oxygen and nickel atoms was confirmed by the EDX test. The magnetic properties results showed that nanoNiO had a narrow hysteretic loop. It consumed the least amount of energy and, therefore, can be used as a core for electric motors and transformers.

Keywords: NiO nanoparticles, Williamson-Hall, XRD, Structural Properties, magnetic properties

1. Introduction

The study of microscopic particles is gaining popularity due to the novel features that materials exhibit as their crystal size is reduced [1]. This is because of their wide variety of usages, such as solar cells [2], supercapacitors [3], electrochemical applications [4], and gas sensors [5]. NiO nanoparticles are among the generality of promising metal oxide nanoparticles [6]. Given the unique features of nanoscaled materials and their industrial uses, the nano-size impact of magnetism has become a powerful research topic [7]. Nickel oxide (NiO) is a promising material employed in various applications, including battery cathodes, catalysis, electrochromic films, and

gas sensors. Bulk NiO is also antiferromagnetic, making it suitable for a wide range of magnetic applications, including pinning layers in spin valves and magnetic tunnel junctions [8].

The cubic (NaCl-type) structure of bulk NiO has a lattice parameter of 4.177 Å. It's a p-type semiconductor with wide band gap of 3.6 to 4.0 eV. Below, Neel's temperature of TN = 523 K shows antiferromagnetic ordering in the bulk form [9]. NiO nanoparticles' magnetic characteristics are susceptible to the crystal structure, size, and shape, resulting in a wide range of fascinating occurrences [10].

Nickel oxide (NiO) is one of the best metal oxides, with key qualities such as large specific capacitance, broadband gap, steady durability, and high carrier density. These characteristics are ideal for dye-synthesized solar cells, electrochromic devices, lithium-ion batteries, and other applications. Furthermore, ferromagnetism in NiO thin films at ambient temperature and its use in spintronic devices [11].

Depending on the size of the nanoparticles, nickel oxide (NiO) with a Neel temperature of 523 K shows varied magnetic characteristics such as ferromagnetism, antiferromagnetism, and superparamagnetism [12]. Nickel oxide (NiO) is a transition metal oxide with cubic crystal structure and p-type conductivity with a direct wide band gap in the range of (3.6 to 4.0) eV [8]. With the highest Neel temperature of 524K, NiO exhibits type-II antiferromagnetic (AFM) order. [13] Chemical and physical methods [14], such as the co-precipitation method [15], solvothermal [16], and sol-gel method [17], have all been used to make NiO NPs. Co-precipitation is one of the simplest techniques for producing nanoparticles among the different approaches. The co-precipitation approach lowers the temperature of the reaction by precipitating a homogenous mixture of reagents. It is a simple way to make nanopowders of metal oxides that are highly reactive in low-temperature sintering [18].

In this research, we will discuss the effect of the crystal structure and grain size on the magnetic properties of nano nickel oxide prepared by the precipitation method.

2. Experimental Method

The Nickel oxide nanoparticles were prepared by the precipitation technique in the following steps:

10.541g aqueous nickel sulfate $NiSO_4.6H_2O$ dissolved in 200 ml of deionized water. 3.1998 g of sodium hydroxide NaOH was dissolved in 400mL of deionized water. The mentioned solution was mixed for 30 minutes at room temperature. After that, the acidity function of the pH solution was modified by using a pH meter by adding ammonia solution NH3 drop by drop until we reached to11 and the color of the solution became blue. After that step, the solution was heated to 800 ℃ for 2 hours. The drops of dissolved sodium hydroxide were slowly added to the solution until the solution became colorless with a green precipitate. The formed precipitate was separated using filter paper with small pores and washed several times with deionized water. Finally, the precipitate was placed in an oven to dry at a temperature of 110 ℃ for 24 hours. The nano compound was placed in the electric furnace at a temperature of 450 ℃ for four hours and then left to cool down to get the nano powder of NiO.

3. Results and Discussion
3.3. X-Ray Diffraction

The XRD patterns of the produced samples clearly reveal the cubic NiO characteristic peaks at 37.3426.43.3745, 62.9490, 75.4857, and 79.4885, which correspond to crystal planes (111), (200), (220), (311), and (222) respectively. The sample's diffraction pattern corresponds to the face-centered cubic (FCC) crystalline structure of NiO, which matches the standard JCPDS card no.04-0835[19]. No impurity peaks are noticed, indicating that the NiO samples are of excellent purity as manufactured.
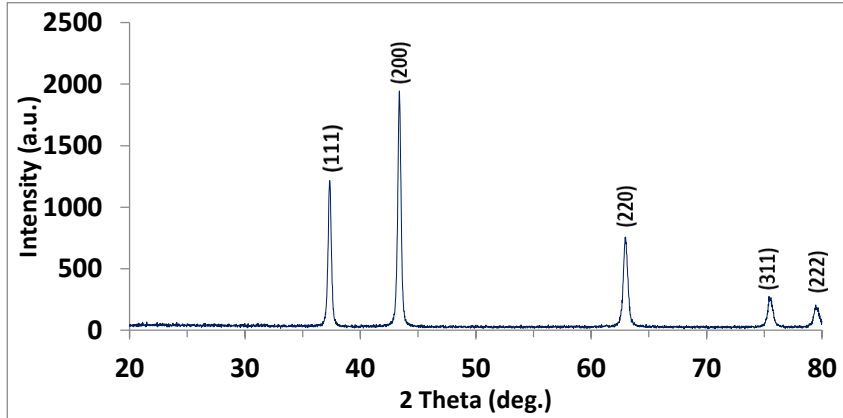

Figure 1: X-ray diffraction pattern of NiO nanoparticles prepared by precipitation method.

The software "fullprof" is used to calculate the lattice constant and theoretical density of nickel oxide nanoparticles is calculated by the following relation [20] and the result is shown in Table 1.

$$\rho = \frac{8\ M_w}{N_A.a^3} \quad \text{……………………….. (1)}$$

Where, M_w: the molecular weight, N_A: Avogadro's number, a: lattice constant.

Crystallite size

The average crystal size of the samples prepared by the precipitation method of nickel oxide nanoparticles is calculated according to Scherrer equation [21, 22]:

$$D = \frac{K\lambda}{\beta cos\theta}$$

By adding the term $\varepsilon = \frac{\beta_S}{tan\theta}$,which represents the micro strain to the Scherrer equation, the equation becomes in the following form and is called the Williamson-Hall equation [23,24]:

$$\beta_{hkl} = \beta_s + \beta_D \quad \text{………………… (2)}$$
$$\beta_{hkl} = \frac{k\lambda}{Dcos\theta} + 4\varepsilon tan\theta \quad \text{………………… (3)}$$
$$\beta_{hkl}cos\theta = \frac{k\lambda}{D} + 4\varepsilon sin\theta \quad \text{……………….(4)}$$

D: crystal size (nm). K: shape factor. λ: the wavelength of X-rays. βhkl: maximum width at mid intensity (FWHM). θ: the angle of incidence of X-rays (Bragg angle). ε :micro strain. The results are shown in **Figure 2** and **Table 1**.
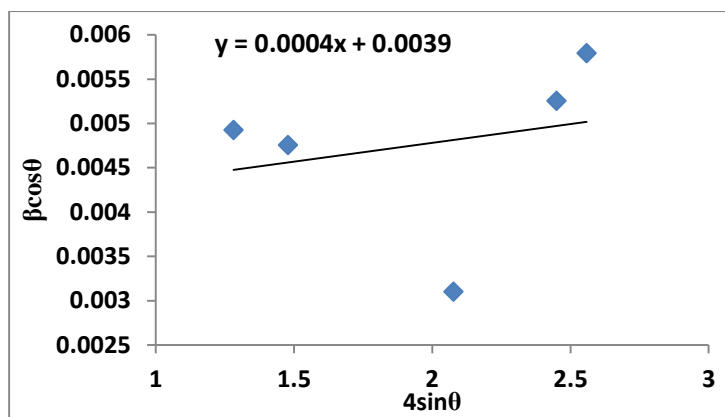
$$y = 0.0004x + 0.0039$$

Figure 2: Plot of W-H analysis of NiO nanoparticles prepared by precipitation method.

It is a property of the material and has great importance, as it is possible to know the properties and type of the material from this value, as the smaller the size of the nanoparticles, the larger the surface area. The surface area is calculated in the following relationship [25.]:

SA=6000/D ρ   …………………………… (5)

SA: surface area (m^2/g). D: particle size (nm).   ρ: the density of the material (g/cm^3).
The results are shown in Table 1.

Crystallization Factor

It is one of the important indicators by which it is possible to know if the sample is monocrystalline or polycrystalline based on X-ray diffraction data. It is calculated according to the following relationship [26, 27]:

$$I_{cry} = \frac{D(AFM,SEM)}{D_{XRD}}$$ ……………………………. (6)

I_{cry}: Crystallization coefficient. D: crystal size from AFM scan or SEM.
D $_{XRD}$: crystal size using Scherer equation.

If the value of the crystallization coefficient is equal to one, then the crystal is monocrystalline, but if its value is greater than one, then the substance is polycrystalline [28]. The results are as shown in **Table 1**.

Table 1: Some of structural parameters of NiO nanoparticles prepared by precipitation method.

a (Å)	ρ (g/cm^3)	D$_{SH}$ (nm)	D$_{W-H}$ (nm)	Micro Strain	SA$_{W-H}$ (m^2/g)	SA$_{SH}$ (m^2/g)	I$_{cr}$
4.17834	6.80112	30.5	35.5	4x10^{-4}	24.82	28.96	1.82

The "Powdercell" software was used to calculate the length of the ionic bond between the two atoms of oxygen and nickel in the crystal lattice. The results were included in **Table (2). T**he angles between them were calculated, and the results were included in **Table (3).**

Table 2: The length of bonds between Ni-O nanoparticles prepared by precipitation method.

atom1	atom2	Bond length (Å)	Bond number
Ni	O	2.9543	2
O	Ni	2.9873	2
O	O	4.2069	1

Table 3: The angles between Ni-O nanoparticles prepared by precipitation method.

atom1	atom2	atom2	Angle	Angle number
Ni	O	Ni	172.0	2
Ni	O	O	82.91	1
O	Ni	O	85.90	1

3.2. Texture Coefficient

It is a description and measure of the degree of the best orientation ratio between crystalline planes and can be calculated using the Harris method according to the following equation [29]:

$$ \text{TC}_{hkl} = \frac{I_{hkl}/I\circ_{hkl}}{\frac{1}{N}\Sigma_N \, I_{hkl}/I\circ_{hkl}} \quad\text{...... ....} \quad (7) $$

N: the number of apparent peaks in the X-ray diffraction pattern.

I_{hkl}: the measured relative intensity.

I_o : the standard intensity of the plane (hkl) from the (JCPDS) card[29].

It can be noticed from the obtained values that there is the highest and best growth of nanoparticles for the samples prepared along the planes (311) and (200). Due to its high formation energy, the lack of growth is at other planes, and the lowest growth is at the plane (111). In general, if TC≅1, then this indicates that the planes' crystal growth is in random directions. This is in good agreement with the JCPDC index [30], but if TC>1 indicates a preferred orientation, and if TC<1, it is polycrystalline, meaning there is a lack of growth Crystal surfaces [31,32], and the results are shown in **Table 4.**

Table 4: The value of angles between Ni-O nanoparticles prepared by precipitation method.

TC (111)	TC (200)	TC (220)	TC (311)	TC (222)
0.77	1.16	0.83	1.01	0.79

3.3. Dislocation Density

Dislocations that occur in the structure of the crystal strongly affect the properties of the material and represent the number of dislocation lines per unit volume of the crystal, and the dislocation density can be calculated according to the following equation [33]:

$$ \delta = \frac{15\beta_{hkl}\cos\theta}{4aD} \quad\text{..} \quad (8) $$

δ: intensity of dislocations. D: crystal size (nm). a : lattice constant (Å).

β_{hkl}: maximum width at mid intensity (FWHM). θ: the angle of incidence of X-rays (Bragg angle).

Crystal defects are formed during the crystal growth process, and it is difficult to get rid of impurities and defects in the crystal, and the presence of defects is sometimes an advantage. Among those crystals, defects are dislocations; the dislocation density of samples is calculated for each plane and the results are shown in **Table (5).**

Table 5: The Dislocation Density ofNi-O nanoparticles prepared by precipitation method.

$\delta_{(111)} *10^{14}$ (m^{-2})	$\delta_{(200)} *10^{14}$ (m^{-2})	$\delta_{(220)} *10^{14}$ (m^{-2})	$\delta_{(311)} *10^{14}$ (m^{-2})	$\delta_{(222)} *10^{14}$ (m^{-2})
15.715	14,647	6.236	17.876	21.732

3.4. Magnetic Properties

A vibrating-sample magnetometer (VSM) was used to measure the magnetic characteristics. Because of the odd electron present, nitric oxide has a paramagnetic property (unpaired electron). When this electron is lost, the diamagnetic NO+ is created. The relationship between the magnetic flux (B) and the intensity of the applied magnetic field (H) is one of any magnetic material's most important magnetic properties. It is represented by the hysterical loop (B-H loop), which is a measure of the energy lost per unit volume during one magnetization cycle. The chemical composition affects the shape and width of the hysterical loops. Figure (3) shows the magnetization curves of the NiO nanoparticles for the sample prepared by the deposition method. We notice that the hysterical loop is narrow. From Table (6), it is noted that the highest saturation is 0.085 emu/g.

Furthermore, the samples having the least area for the retardation ring means that they consume the least energy and, therefore, can be used as cores for electric motors and transformers because they have the lowest magnetic loss [34]. The large surface area compared to the volume of nanomaterials, interfaces, defects, and oxygen vacancies make the magnetic properties of nanoscaleNiO very complex [35]. In addition, it was found that NiO nanoparticles' magnetic characteristics are strongly influenced by particle size [36].
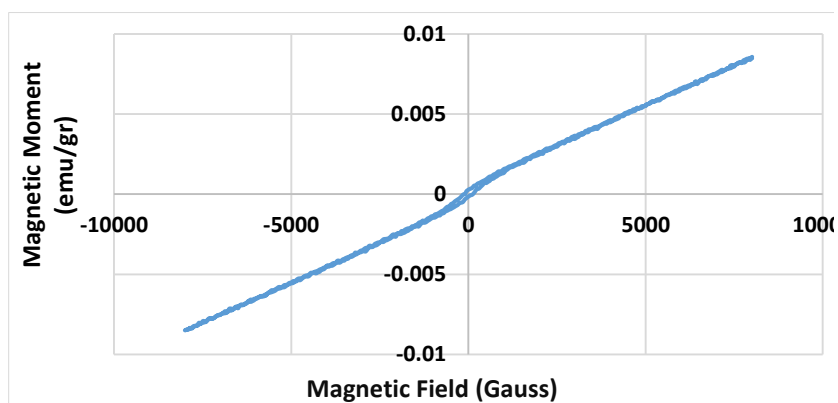

Figure 3: magnetization versus magnetic field ofNi-O nanoparticles prepared by precipitation method.

Table 6: values of magnetic properties ((Hc, Hs, μs) ofNi-O nanoparticles prepared by precipitation method.

Hc (Oe)	**Hs** (Oe)	**μs** (emu/g)
-100	8000	0.085

3.5. Field Emission-Scanning electron microscope (FE-SEM) analysis

The scanning electron microscope (SEM) technique is used to photograph the samples for the purpose of knowing the details of the sample's surfaces and knowing the shape, size, and degree of homogeneity of the samples. SEM images are magnified at 135 kX, and Figure 4 shows the morphology and average particle size present in the samples of NiO NPs prepared by the deposition method. The SEM image shows that the particle shape has a ball-like appearance with a uniform and homogeneous distribution.
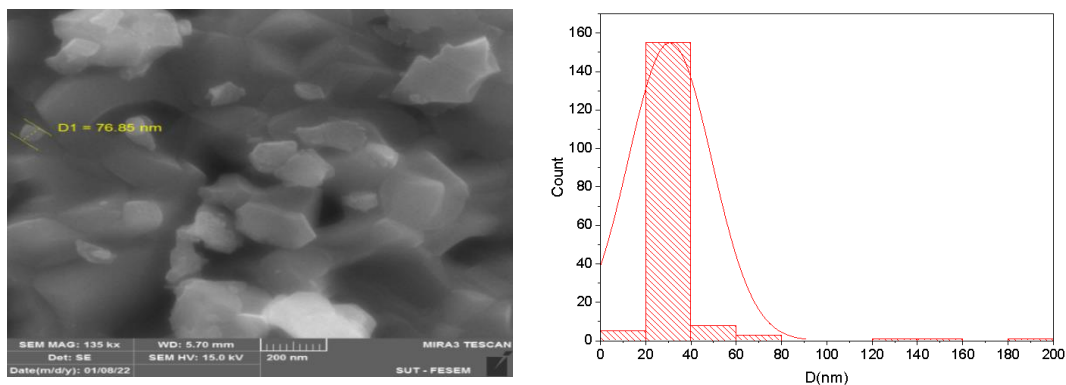

Figure 4: SEM micrographs of nickel oxide nanoparticles.

3.6. Energy Dispersive X-ray (EDX)

The elements of the prepared nanoparticles can be identified using EDX spectroscopy, which measures the energy difference between the two outer shells and the element's atomic structure. The EDX spectrum of NiO NPs shows the peaks corresponding to Ni and O, as shown in Figure 5. The reason for the presence of C is the residue of the combustion reaction, and the presence of Pt is one of the characteristics of the device, as the sample is coated with a layer of Pt to increase the conductivity [37]. In addition, the appearance of sulfur S as an impurity in the sample is very small percentage due to the use of nickel sulfate as raw materials in the deposition method. The peaks of the nickel element appear with three energies at (Kα, Lα) and its quantity Kα = 7.480 keV, Lα = 0.849 keV, and the peak of the oxygen element is shown at the site Kα = 0.525 keV.
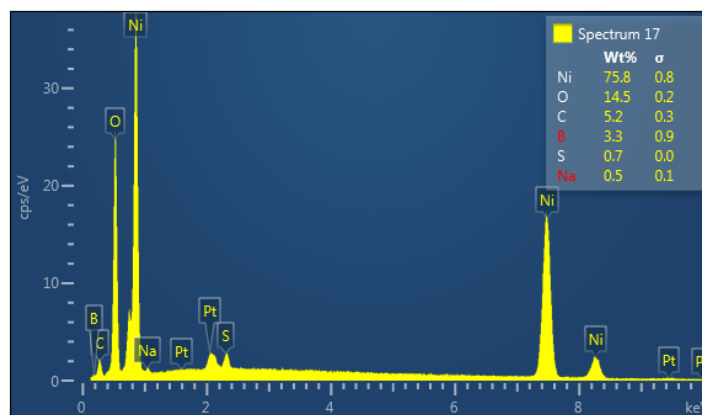

Figure 5: EDX spectroscopy of nickel oxide nanoparticles.

4. Conclusion

The nickel oxide (NiO) nanoparticles were prepared in a low-cost method by precipitation technique. The aqueous nickel sulfate $NiSO_4.6H_2O$ and NaOH were used as precursors. NiO has a face-centered cubic (FCC) structure with a crystallite size of (30.5-35.5) nm, a lattice constant of 4.17834 Å, and a theoretical density of 6.80112 g/cm^3 according to the XRD pattern. The magnetic hysteresis of the studied NiO nanoparticles displayed that it has magnetic properties. The hysteretic ring is narrow, and the highest saturation is 0.085 emu/g. The samples with the least area of the hysteresis loop mean that they consume the least energy and, therefore, can be used as the core of electric motors and transformers because they have the least magnetic loss.

References

1. Tiwari, S. D.; Rajeev, K. P. Magnetic properties of NiOnanoparticles, *Thin Solid Films*, **2006**,*505*(*1-2*), 113-117.
2. Ukoba, K. O.;Eloka-Eboka, A. C.;Inambao, F. L. Review of nanostructured NiO thin film deposition using the spray pyrolysis technique. *Renewable and Sustainable Energy Reviews*,**2018** ,*82*, 2900-2915.
3. Han, D.; Jing, X.; Wang, J.;Yang, P.; Song, D.; Liu, J. Porous lanthanum doped NiO microspheres for supercapacitor application. *Journal of electroanalytical chemistry*,**2012**,*682*, 37-44.
4. Soomro, R. A.;Ibupoto, Z. H.;Abro, M. I.;Willander, M. Controlled synthesis and electrochemical application of skein-shaped NiO nanostructures. *Journal of Solid State Electrochemistry*, **2015**,*19*(*3*), 913-922.
5. Arif, M.;Sanger, A.; Singh, A. Highly sensitive NiO nanoparticle based chlorine gas sensor. *Journal of Electronic Materials*,**2018**, *47*(*7*), 3451-3458.
6. Al Boukhari, J.;Khalaf, A.;Awad, R. Structural and electrical investigations of pure and rare earth (Er and Pr)-doped NiO nanoparticles. *Applied Physics A*, **2020**,*126*(*1*), 1-16.
7. Karthik, K.;Selvan, G. K.;Kanagaraj, M.;Arumugam, S.; Jaya, N. V. Particle size effect on the magnetic properties of NiO nanoparticles prepared by a precipitation method. *Journal of Alloys and compounds*, **2011**,*509*(*1*), 181-184.
8. Proenca, M. P.; Sousa, C. T.; Pereira, A. M.; Tavares, P. B.;Ventura, J.; Vazquez, M.;Araujo, J. P. Size and surface effects on the magnetic properties of NiO nanoparticles. *Physical Chemistry Chemical Physics*,**2011**, *13*(*20*), 9561-9567.
9. Tadic, M.;Nikolic, D.;Panjan, M.; Blake, G. R. Magnetic properties of NiO (nickel oxide) nanoparticles: Blocking temperature and Neel temperature. *Journal of Alloys and Compounds*,**2015**, *647*, 1061-1068.
10. Duan, W. J.; Lu, S. H.; Wu, Z. L.; Wang, Y. S. Size effects on properties of NiO nanoparticles grown in alkalisalts. *The Journal of Physical Chemistry C*,**2012**, *116*(*49*), 26043-26051.
11. Patil, R. A.;Devan, R. S.; Lin, J. H.; Ma, Y. R.;Patil, P. S.;&Liou, Y. Efficient electrochromic properties of high-density and large-area arrays of one-dimensional NiOnanorods. *Solar energy materials and solar cells*,**2013**, *112*, 91-96.
12. Bayappagari, B.;Shaik, K.;Chakraborty, D.;Kunapalli, C. K. Structural, optical and magnetic properties of vacuum annealed Fe, Mn doped NiO nanoparticles. *Applied Physics A*, **2021**,*127*(1), 1-9.
13. Panigrahi, U. K.;Sathe, V.;Babu, P. D.;Mitra, A.;Mallick, P. Effect of Mg doping on the improvement of photoluminescence and magnetic properties of NiO nanoparticles. *Nano Express*, **2020**,*1*(*2*), 020009.
14. Radwan, N. R.; El-Shall, M. S.; Hassan, H. M. Synthesis and characterization of nanoparticle Co_3O_4, CuO and NiO catalysts prepared by physical and chemical methods to minimize air pollution. *Applied Catalysis A: General*,**2007**, *331*, 8-18.

15. Mishra, A. K.;Bandyopadhyay, S.; Das, D. Structural and magnetic properties of pristine and Fe-doped NiO nanoparticles synthesized by the co-precipitation method. *Materials Research Bulletin*,**2012**, *47*(*9*), 2288-2293.

16. Anandan, B.;Rajendran, V. Morphological and size effects of NiO nanoparticles via solvothermal process and their optical properties. *Materials Science in Semiconductor Processing*, **2011**,*14*(*1*), 43-47.

17. Alagiri, M.;Ponnusamy, S.;Muthamizhchelvan, C. Synthesis and characterization of NiO nanoparticles by sol–gel method. *Journal of Materials Science: Materials in Electronics*,**2012**, *23*(*3*), 728-732.

18. Rahman, M. A.;Radhakrishnan, R.;Gopalakrishnan, R. Structural, optical, magnetic and antibacterial properties of Nd doped NiO nanoparticles prepared by co-precipitation method. *Journal of Alloys and Compounds*,**2018** *742*, 421-429.

19. Kim, J. K.; PEG-assisted sol-gel synthesis of compact nickel oxide hole-selective layer with modified interfacial properties for organic solar cells. *Polymers*,**2019** *11*(*1*), 120.

20. Saheb, L.; Al-Saadi, T. M. Synthesis, Characterization, and NH3 Sensing Properties of (Zn0. 7 Mn$_{0.3-x}$Ce$_x$ Fe$_2$O$_4$) Nano-Ferrite. In *Journal of Physics: Conference Series* ,**2021**, December ,*2114, 1*, 012040. IOP Publishing.

21. Al-Saadi, T. M.;Abed, A. H.;Salih, A. A. Synthesis and Characterization of Al$_y$Cu$_{0.15}$Zn$_{0.85-y}$Fe$_2$O$_4$ Ferrite Prepared by the Sol-Gel Method. *Int. J. Electrochem.Sci*,**2018**, *13*, 8295-8302.

22. Al-Kalifawi, E. J.; Al-Obodi, E. E.; Al-Saadi, T. M. Characterization of Cr$_2$O$_3$ nanoparticles prepared by using different plant extracts. *Acad. J. Agric. Res*,**2018**, *6*, 026-032.

23. Abed, A. H.;Khodair, Z. T.; Al-Saadi, T. M.; Al-Dhahir, T. A. Study the evaluation of Williamson–Hall (WH) strain distribution in silver nanoparticles prepared by sol-gel method. In *AIP Conference Proceedings,* **2019**, July,*2123, 1*, 020019. AIP Publishing LLC.,

24. Ahmed, O. A.; Abed, A. H.; Al-Saadi, T. M. Magnetic Properties and Structural Analysis of Ce-Doped Mg–Cr Nano-Ferrites Synthesized Using Auto-Combustion Technique. In *Macromolecular Symposia* ,**2022**, February ,*401, 1*, 2100311.

25. Al-Saadi, T. M.;Alsaady, L. J. Preparation of Silver Nanoparticles by Sol-Gel Method and Study their Characteristics. *Ibn AL-Haitham Journal For Pure and Applied Science*, **2017**,*28*(*1*), 301-310.

26. Al-Dahair, T. A.; Al-Mahdawy, M. E. Influence of Doping on K2SO4 Crystal Properties. *Ibn Al-Haitham Journal for Pure and Applied Science*, **2015** ,*28*(*1*).]

27. Li, Z.;Hou, B.;Xu, Y.; Wu, D.; Sun, Y.; Hu, W.; Deng, F. Comparative study of sol–gel-hydrothermal and sol–gel synthesis of titania–silica composite nanoparticles. *Journal of Solid State Chemistry*, **2005**,*178*(*5*), 1395-1405.

28. Roy, R.; Ceramics by the solution-sol-gel route. *Science*, **1987** ,*238*(*4834*), 1664-1669.

29. Niederberger, M.; Pinna, N. Aqueous and nonaqueous sol-gel chemistry. *Metal oxide nanoparticles in organic solvents: Synthesis, formation, assembly and application*,**2009,** 7-18.

30. Hale, P. S.; Maddox, L. M.;Shapter, J. G.;Voelcker, N. H.; Ford, M. J.;Waclawik, E. R. Growth kinetics and modeling of ZnO nanoparticles. *Journal of Chemical Education*,**2005** *82*(*5*), 775.

31. Van Dong, P.; Ha, C. H.;Binh, L. T.;Kasbohm, J. Chemical synthesis and antibacterial activity of novel-shaped silver nanoparticles. *International Nano Letters*,**2012** ,*2*(*1*), 1-9.

32. Kumar, M. S.;Soundarya, T. L.;Nagaraju, G.; Raghu, G. K.;Rekha, N. D.;Alharthi, F. A.;Nirmala, B. Multifunctional applications of Nickel oxide (NiO) nanoparticles synthesized by facile green combustion method using Limoniaacidissima natural fruit juice. *InorganicaChimicaActa*, **2021**,*515*, 120059.

33. Parashar, M.;Shukla, V. K.; Singh, R. Metal oxides nanoparticles via sol–gel method: a review on synthesis, characterization and applications. *Journal of Materials Science: Materials in Electronics*,**2020** *31*(*5*), 3729-3749.

34. Sabouri, Z.;Akbari, A.;Hosseini, H. A.; Khatami, M.;Darroudi, M. Green-based bio-synthesis of nickel oxide nanoparticles in Arabic gum and examination of their cytotoxicity, photocatalytic and antibacterial effects. *Green Chemistry Letters and Reviews*,**2021** ,*14*(*2*), 402-412.

35. Xu, J.; Yang, H.; Fu, W.; Du, K.; Sui, Y.; Chen, J.;Zou, G. Preparation and magnetic properties of magnetite nanoparticles by sol–gel method. *Journal of Magnetism and magnetic Materials*,**2007** ,*309*(*2*), 307-311.

36. Karthik, K.;Selvan, G. K.;Kanagaraj, M.;Arumugam, S.;& Jaya, N. V. Particle size effect on the magnetic properties of NiO nanoparticles prepared by a precipitation method. *Journal of Alloys and compounds*, **2011**, *509*(1), 181-184.

37. Gondal, M. A.;Saleh, T. A.;Drmosh, Q. A. Synthesis of nickel oxide nanoparticles using pulsed laser ablation in liquids and their optical characterization. *Applied Surface Science*,**2012** ,*258*(*18*), 6982-6986.